

# Effect of crystal size on the tribological behavior of manganese phosphate coatings under lubricated sliding

Proc IMechE Part J:  
J Engineering Tribology  
0(0) 1–8  
© IMechE 2017  
Reprints and permissions:  
sagepub.co.uk/journalsPermissions.nav  
DOI: 10.1177/1350650117749485  
journals.sagepub.com/home/pij



Nicolás S Fochesatto<sup>1</sup>, Camila Müller<sup>2</sup>, Nicolás A Zabala<sup>1</sup>,  
Pablo A Castro<sup>3</sup> and Walter R Tuckart<sup>1</sup>

## Abstract

In this study, the wear and friction behavior of manganese phosphate coatings with different crystal sizes were investigated. Crystal size was controlled modifying the chemical composition of the phosphating bath, particularly the concentration of the activator which modifies the number of nuclei for crystal growth. Activator concentration range used for this work varied from 0 to 0.7 g/L, and crystal size was measured using image analysis software on scanning electron microscopy photographs. Available volume for lubricant retention was determined measuring the phosphated surface with a 3D optical profilometer. At the same time, lubricated wear tests were carried out using a ring-on-block configuration at low speeds (23 mm/s) and high loads (14,500 N). Wear behavior was determined as the sliding distance to failure, which was noticed through signs of removal of the phosphate along with the increase of coefficient of friction. It was found that there is a competition between the availability of volume to hold the lubricant, which increases with the crystal size, and the surface coverage, which diminishes as the crystal size grows. Optimal results were obtained for an activator concentration of 0.3 g/L, which meant an average crystal size of 16  $\mu\text{m}$ .

## Keywords

Manganese phosphate coatings, ring on block, galling, crystal size

Date received: 28 July 2017; accepted: 19 November 2017

## Introduction

Manganese phosphate coatings are commonly used to reduce friction when combined with suitable lubricants. These coatings have been applied to cast iron<sup>1</sup> and steel substrates<sup>2</sup> to reduce wear. They are extensively used in components such as gears, camshafts, oil pumps, valves, bearings, pistons, connecting rods, crankshafts, and armament parts.<sup>3,4</sup> These coatings also provide resistance to corrosion, which makes them suitable for aggressive environments.<sup>5</sup> In particular, these coatings are applied to the unions in tubing connections of oil and gas industry.<sup>6</sup>

Manganese phosphate coatings are produced by chemical conversion with Hureaulite ( $\text{Mn, Fe}_5\text{H}_2(\text{PO}_4)_2$ ) as the main component. The literature indicates that they possess excellent lubricity and anti-scratch properties,<sup>1,7,8</sup> their main function being to provide anti-galling properties and lubricant retention, improving the ease of sliding and reducing wear associated with steel surfaces under sliding contact. Its porous structure allows it to absorb oil, providing lubrication between surfaces to prevent mechanical seizure. However, manganese phosphate coatings are

not sufficient for use under dry conditions, as they have no intrinsic lubricating properties.<sup>3,9–11</sup>

Kozłowski and Czechowski<sup>12</sup> investigated the effect of various pretreatments of the base material before applying the manganese phosphate coating and concluded that they significantly extended life under poor lubrication conditions due to their ability to absorb lubricants. Weight loss went from 34 mg, for the unphosphated specimen, to 0.5 mg in the phosphated one.

Many researches have evaluated manganese phosphate coatings using pin-on-disc tests, such as Perry and Eyre,<sup>9</sup> who concluded that a thin fine-grained

<sup>1</sup>Departamento de Ingeniería, Universidad Nacional del Sur, Bahía Blanca, Argentina

<sup>2</sup>PLAPIQUI, Universidad Nacional del Sur – CONICET, Bahía Blanca, Argentina

<sup>3</sup>Department of Surface Chemistry and Coatings, TENARIS, Research and Development Centre, Campana, Argentina

## Corresponding author:

Nicolás S Fochesatto, Departamento de Ingeniería, Universidad Nacional del Sur, Av. Alem 1253, 8000, Bahía Blanca, Argentina.  
Email: nicolas.fochesatto@uns.edu.ar

coating has a better wear performance than a thicker coarser-grained one, i.e. a 30% decrease in the coefficient of friction was found for this case. Ilaiyavel and Venkatesan<sup>11,13,14</sup> studied the application of this coatings to AISI D2 steels with different heat treatments, and they determined that the coefficient of friction was very low when the samples were annealed after phosphating. Ernens et al.<sup>6</sup> investigated the application of phosphate coatings in the make-up of casing connections, concluding that not only good anti-galling response was obtained but also sealability due to the wear of the initial rough surface of the coating.

The articles of Hivart et al.<sup>7,8</sup> are of the few, which tried to correlate the coatings morphology with their tribological characteristics. They used a sliding cylinder against a rotating specimen for a friction-seizure test, and the obtained results were associated with the treatment parameters, which modified the final structure of the coating. The authors concluded that a finer structure implies higher seizure resistance. However, they explain this behavior considering the surface coverage only, and nothing is said about the lubricant-retaining capacity of the coating.

As far as the authors know, none of the mentioned articles, or any other work in the open literature, takes into account the changes in the coating's wear and friction behavior as a consequence of the lubricant retaining capacity caused by the crystal size and surface coverage of the manganese phosphate.

The present work aims to determine the tribological behavior of manganese phosphate coatings focusing on the effect that the coating's crystal size has on the wear resistance and friction. These results were correlated with the available volume in the coating to retain lubricant, which was measured by topographical profiles using an optical profilometer. To accomplish this objective, a ring-on-block lubricated test was used to evaluate the coatings under high contact pressures and low sliding speed.

## Materials and methods

### Base material

The material used as substrate for the coatings, and as counter body, was an API grade L80 steel (wt%: 0.20 C%, 1 Cr%, 0.59 Mn%, 0.49 Mo%, 0.29 Si%, 0.033 Nb%, 0.009 P%, 0.001 S%, and Fe balance) manufactured by TenarisSiderca (Campana, Argentina). It is a material commonly used in the gas and oil industry, e.g. for casings, in combination with the manganese phosphate coatings. Chemical composition was obtained using an optical emission spectrometer. The hardness of the steel was determined to be 231 HV.

### Application of coatings

Before proceeding with the application of phosphate coating, the samples were polished to a surface

roughness  $R_a = 0.1 \mu\text{m}$  with 500-grit sandpaper. Then, phosphate coating was applied through the following steps:

- **Degreasing and rinse:** The test pieces were degreased by 15 min immersion in a weak alkaline solution (60 g/L) at 83 °C. Then, the solution was removed manually by water immersion.
- **Surface activation:** This step was aimed to generate nuclei for crystal growth. It was performed by immersion in a solution of commercial activator (colloidal suspension manganese phosphate) at 40 °C for 1 min with stirring. The concentration of the activator in the bath is fundamental for modifying the properties of the obtained coatings, as it changes the number of nuclei for crystal growth.
- **Phosphatization:** The activated samples were immersed in commercial phosphating solution composed of phosphoric acid, manganese phosphate, and accelerators, at 99 °C for 10 min. The starting and finishing of the reaction is determined by the presence of hydrogen gas in the solution (which can be denoted by bubbles in the solution). After removing the specimens from the phosphating bath, they were rinsed with water and blow-dried with hot air.

### Characterization of coatings

The size of phosphate crystals and the degree of surface coverage were evaluated by optical (Microscope HIROX<sup>®</sup>, model KH-7700) and scanning electron microscopy (SEM, microscope Philips<sup>®</sup>, model XL 30 CP) in the center of research and development at TenarisSiderca (CINI). Crystals were measured from SEM images the Software ImageJ<sup>®15,16</sup> as in the example presented in Figure 1(a). The characteristic size of crystal for each bath concentration was taken as the average of those measured. On the other hand, thickness of the obtained coatings was measured from the SEM images of cross-section of phosphatized rings, using the same software (see Figure 1(b)).

### Determination of available volume

Manganese phosphate coatings have a lubricant retaining capacity due to the volume available between the phosphate crystals.<sup>17</sup>

In order to analyze the effect of phosphate crystals' size in the available volume lubricant, a non-contact 3D optical profilometer Alicona<sup>®</sup> (model Edgemaster) was used to have a precision mapping of the surface topography. After obtaining the surface map, the method used to measure the free volume for lubricant retention can be understood using a concept similar to the Abbott–Firestone curve (bearing area curve).<sup>18–20</sup>

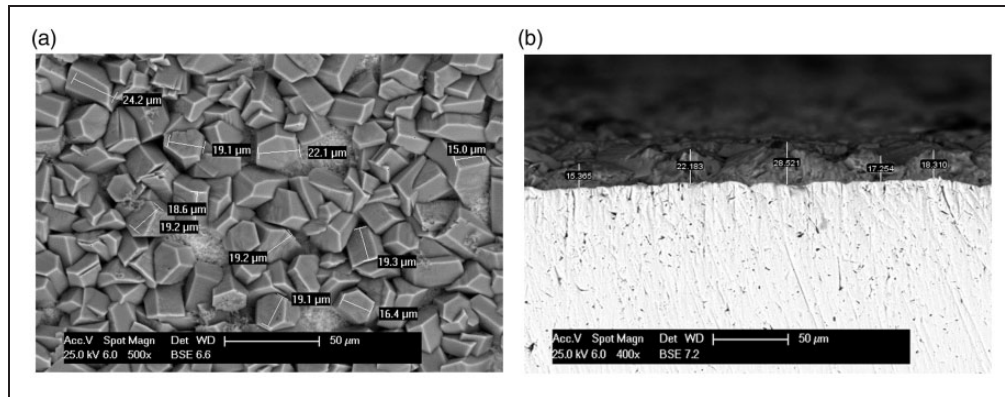


**Figure 1.** (a) Crystal measurement method from a SEM image; (b) thickness measurement from an SEM image of the cross-section.

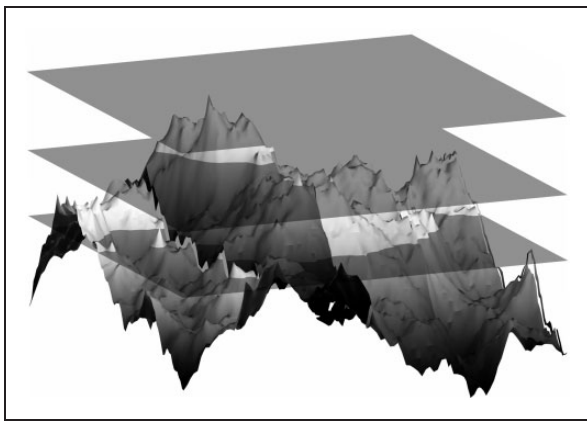


**Figure 2.** Example of rough surface and planes used to evaluate the available volume.

The followed procedure is described next (a qualitative example can be seen in Figure 2):

- The profilometer's output consisted of a file with over a million values corresponding to the spatial coordinates of the points of the measured surface values, which were used to reproduce the 3D surface in MATLAB® Software.<sup>21</sup> The volume between the surface and a plane above it was determined. Then, using a MATLAB® code, the plane was moved, sweeping from the top of the highest peak in the surface to the bottom of it. Figure 3(a) depicts an example of a graph, which associates the height of the plane to the available volume.
- At the beginning of the plane sweeping, there are few peaks and most of the available volume is not capable of retaining lubricant (there are no voids, but empty space). In this first stage, any change in the available volume is explained by the difference in the height of the plane. As the plane moves towards the surface, more peaks are added and the changes in the available volume can be explained by the voids getting smaller. The criteria used to determine the true available volume consisted in taking the turning point in which the

behavior changes. In order to do this, the derivative of the free volume curve was calculated and plotted as a function of the percentage of the height of the highest peak (Figure 3(b)). In the first stage the derivative is almost linearly crescent, while in the second stage, it can be considered constant.

- After selecting the height of the plane at the turning point, the corresponding volume is calculated from the graph of free volume, as shown in Figure 3(a). This procedure was performed several times for each type of coating, in order to obtain an unbiased estimate.

### Wear test

Tribological evaluations were conducted through ring-on-block lubricated test type following the ASTM G77-05 standard,<sup>22</sup> in pure sliding condition under high load and low speed, where the ring is sliding over a fixed block. Figure 4 depicts a schematic representation of the test. This geometric configuration allows limiting the lubricant between the contact surfaces because the block is in nonconforming contact with the ring from the bottom.

The rings and blocks were made of API grade L80 steel. The contact face of the block was polished with a 100-grit sandpaper, giving the surface a roughness value of  $R_a = 1.15 \mu\text{m}$ . Design and nominal dimensions of the test specimens are shown in Figure 5(a). The manganese phosphate coatings were prepared and applied on the specimens. Different kinds of coatings were obtained varying the activator concentration in the bath. The tested values were (in grams per liter of activator concentration): 0; 0.1; 0.2; 0.3; 0.5; and 0.7.

During the tests, the ring rotated at a speed of 11.35 r/min reaching a sliding speed of 23.26 mm/s in the contact area. Applied load was linearly varied from 3800 N to 14,500 N in the first 18 s, and then it was kept at that value until the end of the test, which

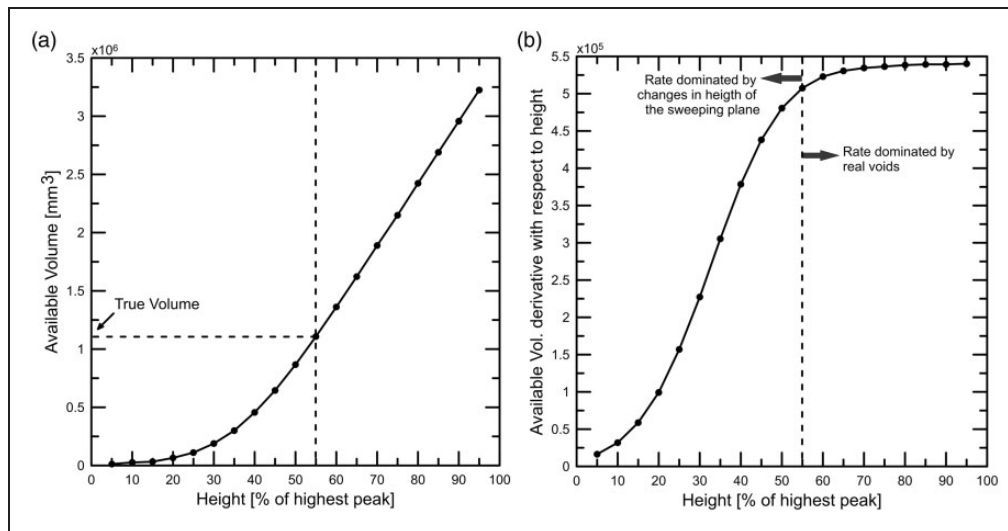


**Figure 3.** (a) Free volume between different planes and the 3D surface for phosphate coating made with a manganese concentration of activator 0.7 g/L; (b) derivative of the free volume.

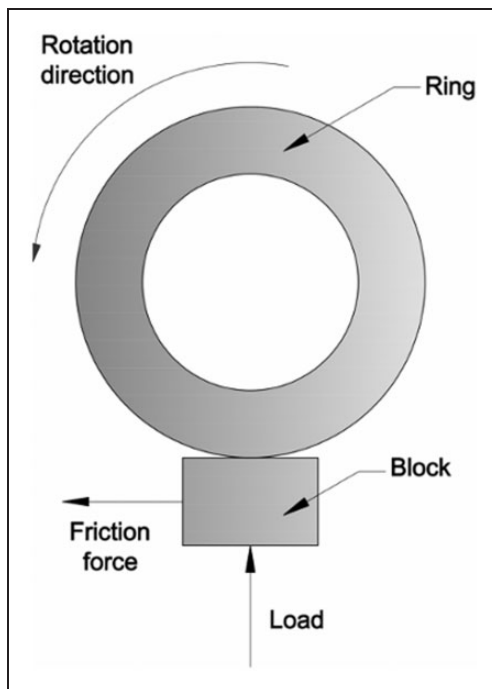


**Figure 4.** Schematic representation of the ring-on-block configuration used in wear tests.

was determined as the moment of failure of the coating and the appearance of galling. Then, the sliding distance until failure could be determined.

Lubrication was achieved by adding grease to the system. The grease used was Bestolife<sup>®</sup> 2010 NM. Ring-on-block tests were carried out under ambient laboratory conditions of 25 °C and a relative humidity of 50%.

The wear behavior was determined as the sliding distance to failure, which was noticed through signs of removal of the phosphate along with the increase of coefficient of friction (COF) and the presence of a

discontinuity in the friction load curve, due to a sudden vibration detected by the load cell when coating failed. Sliding distance could be calculated from the elapsed time since the start of the test until failure.

In the case of friction behavior, COF was used as measurement. An example of COF against time for a coating made from a bath with an activator concentration of 0.3 g/L is shown in Figure 6, where the time at which the coating begins to fail is indicated. COF for each test was taken as the value in which the graph stabilizes.

## Results and discussion

### Characterization of coatings

Significant differences in surface topography were observed in both the size of phosphate crystals and coating uniformity with changes in the activator concentration. The graph presented in Figure 7 shows the results of phosphate crystal size and thickness of the coating depending on the activator concentration. Both variables show a similar trend, which is reasonable considering the fact that crystals grow in all directions.

From the graph in Figure 7, it can be inferred that there is an asymptotic decreasing size ratio of phosphate crystals with increasing activator concentration. This concentration parameter also affects the uncovered surface regions, as can be seen in Figure 8. It was determined that phosphate coatings made with activator concentrations above 0.3 g/L produce good coverage of the entire surface.

### Available volume

Manganese phosphate coatings are well known for retaining lubricant and, therefore, improving the



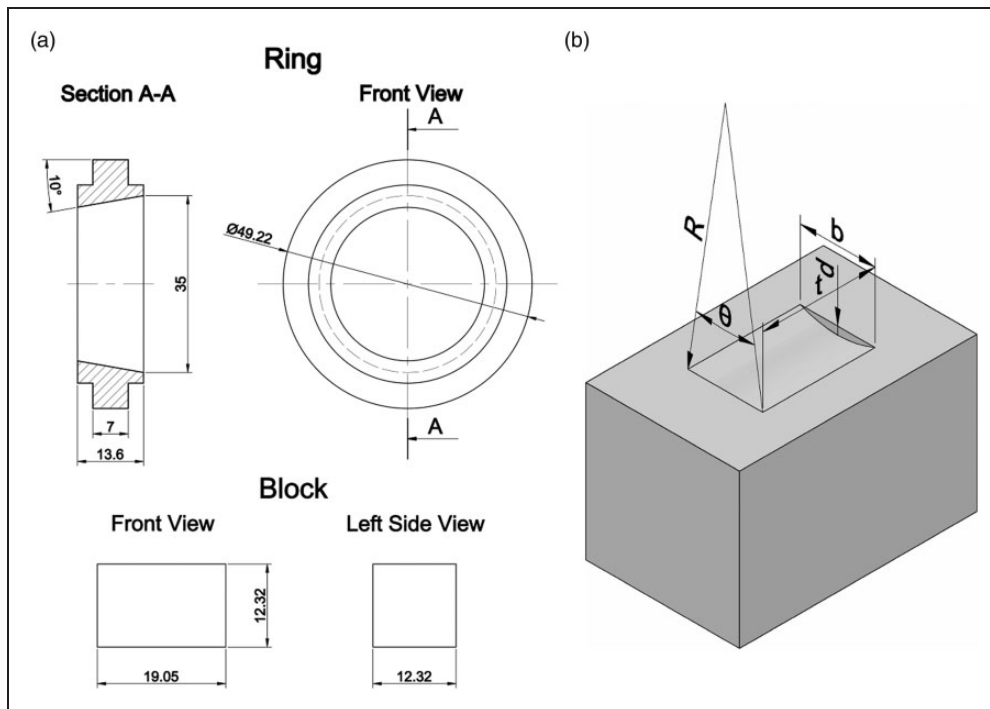


**Figure 5.** (a) Design and geometry of specimens; (b) schematic representation of the scar on the block.

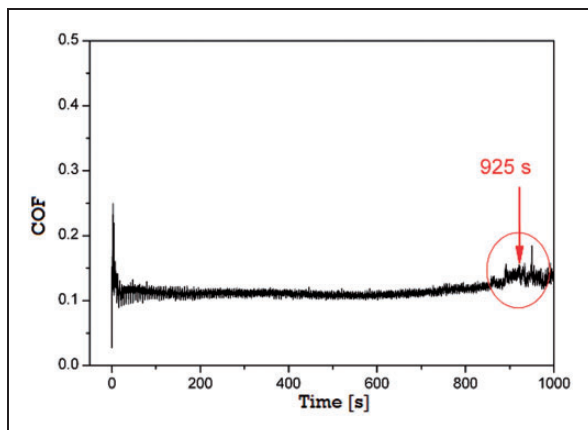


**Figure 6.** Evolution of COF versus time test for activator concentration of 0.3 g/L.

tribological performance. To determine the effect of the size of the phosphate crystals in the volume available to retain lubricant, several coatings were characterized and analyzed using a noncontact 3D optical profiler Alicona<sup>®</sup> and Matlab<sup>®</sup> software,<sup>21</sup> through the technique explained in the “Materials and methods” section. Measurements were made at  $20\times$  magnification, resulting in an observation area of  $1\text{ mm}^2$ . Figure 9 shows the 3D images for different kinds of phosphates.

The results of the volume available according to the activator concentration were obtained. Previously, a correlation between the concentration of activator and the crystal size was established (see Figure 7). Thus, it is possible to determine the

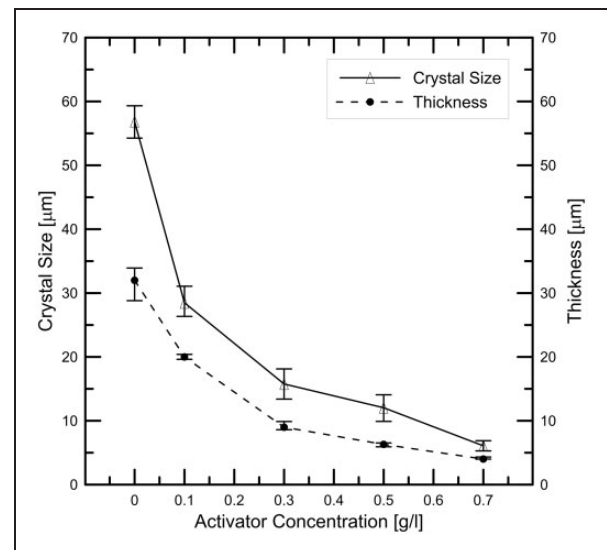


**Figure 7.** Crystal size and thickness versus activator concentration.

relationship between the volume available and the manganese phosphate crystal size as shown in Figure 10.

### Wear behavior

The results of the ring-on-block tests varying the size of phosphate crystal are presented in Figure 11. Each point on the graph corresponds to a group of coated tests carried out with the same type of phosphate rings. The results indicate a maximum performance

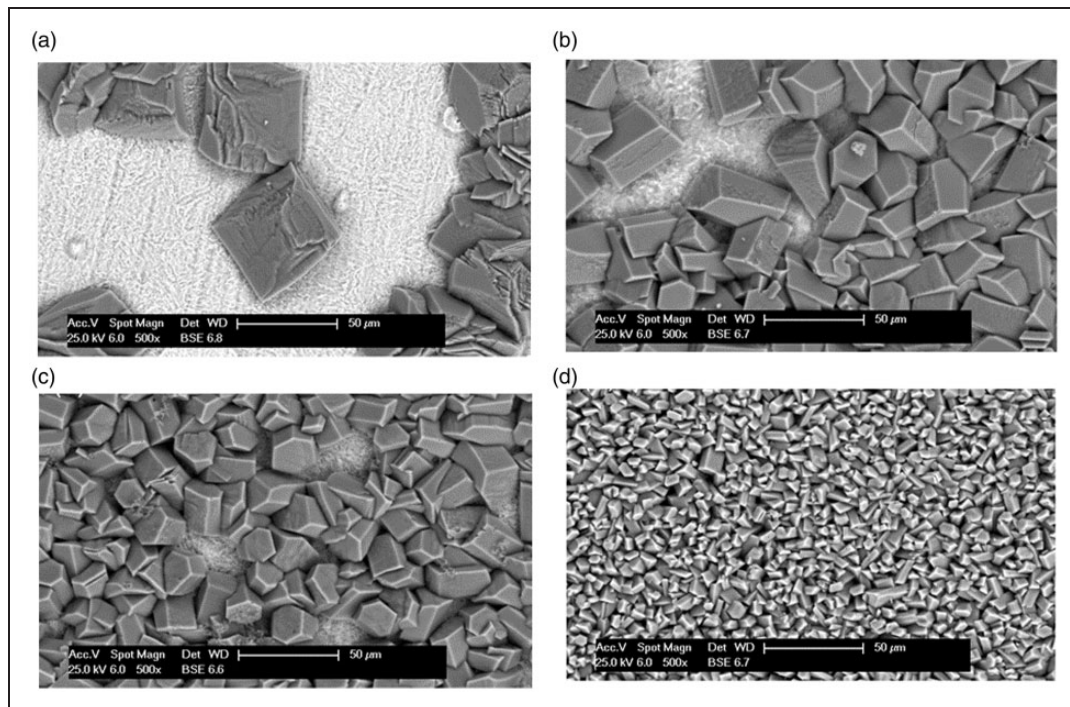


**Figure 8.** SEM images of manganese phosphate coatings with different concentrations of activator: (a) 0 g/L; (b) 0.1 g/L; (c) 0.3 g/L; (d) 0.7 g/L.

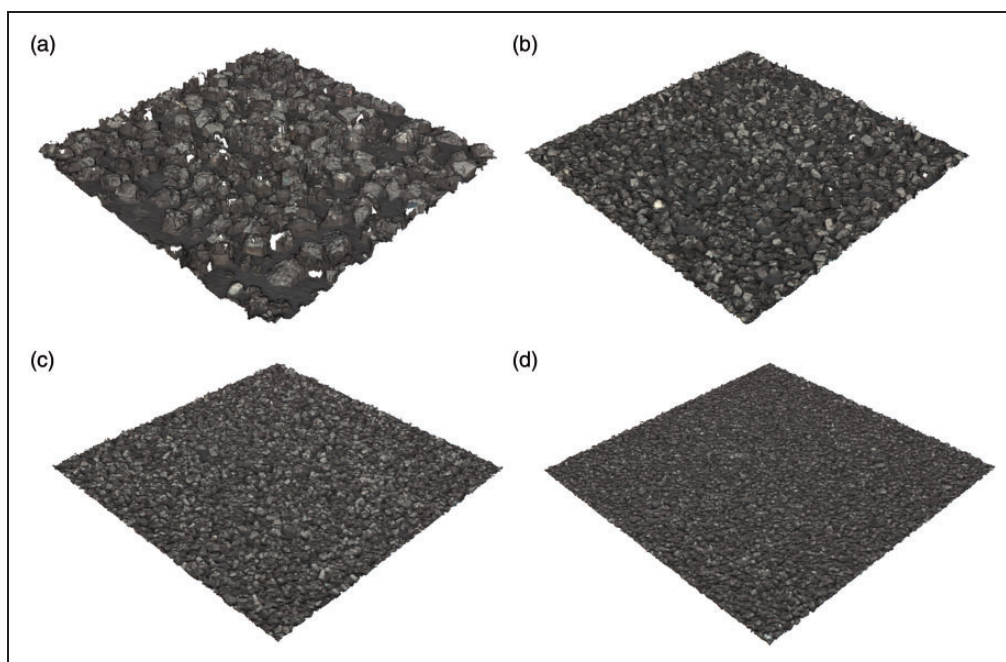


**Figure 9.** 20 × 3D images for different activator concentration: (a) 0 g/L; (b) 0.1 g/L; (c) 0.3 g/L; (d) 0.5 g/L.

for those coatings with an average crystal size of  $16\ \mu$ , corresponding to the coatings made with an activator concentration of 0.3 g/L. Those coatings combine reasonable crystal size with good surface coverage. Coatings with crystal size smaller than  $16\ \mu$  have less lubricant retention (see Figure 10), causing poor lubrication and, consequently, the early coating

deterioration. Those coatings with grain size larger than  $16\ \mu$  had the disadvantage that the phosphatized surface was not completely uniform, leaving areas without phosphate crystals, allowing direct metal-to-metal contact (Figure 11). All tests ended with the detachment of the coatings caused by adhesive wear, and appearance of galling.

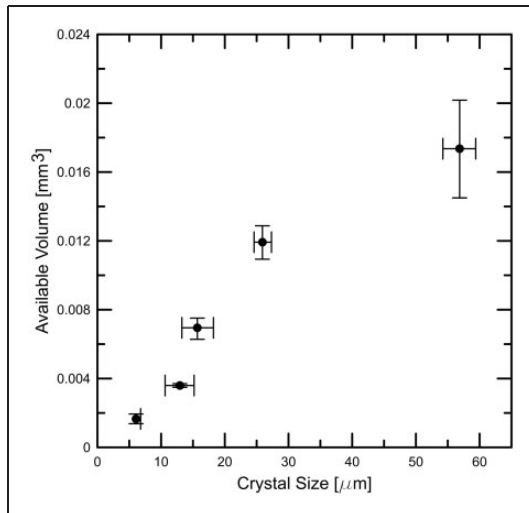


**Figure 10.** Volume available for the lubricant depending on the crystal size (horizontal error bars are due to dispersion in the measurement of crystal size).

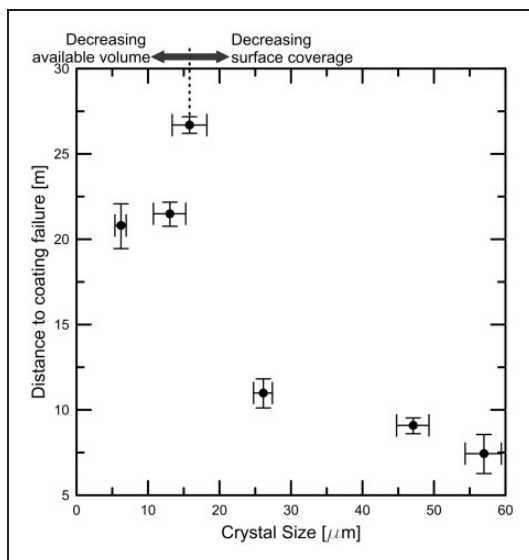


**Figure 11.** Sliding distance until coating failure as a function of the crystal size.

According to Perry and Eyre,<sup>9</sup> very thick manganese phosphate coatings have better performance when sliding against surfaces with large roughness ( $R_a = 1.1 \mu\text{m}$ ), while thin coatings with fine crystals are more suitable if the contacting surfaces are smooth ( $R_a = 0.24 \mu\text{m}$ ). These results are consistent with the results obtained in this work and those obtained in full-scale make and brake tests.

However, other authors<sup>7,17</sup> have reported opposite results, as they concluded that the best wear behavior is obtained by using fine-grained porous coatings. This difference could be attributable to test conditions and type of geometric configurations used by these authors.

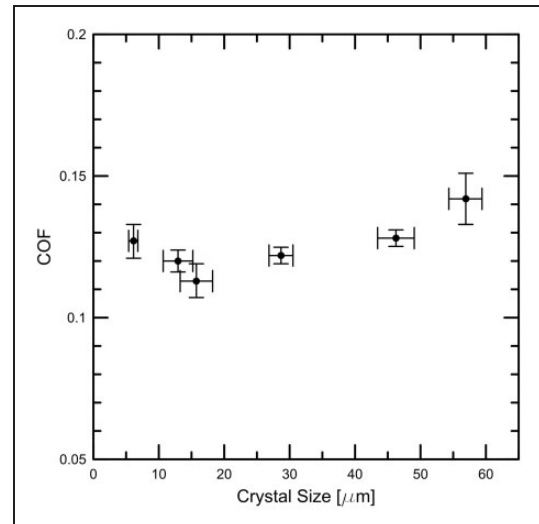


**Figure 12.** Average COF in the stable area according to the size of the phosphate crystal.

**Friction behavior.** The graphs as the one depicted in Figure 6 show a change in the slope of COF at the moment where the coating begins to deteriorate, allowing the metal-to-metal contact. At the beginning of the test, a high COF can be appreciated, which last for about one rotation, and is related to the settlement process. The obtained values of COF are in coincidence with those reported in the literature.<sup>11,23</sup> Figure 12 depicts the average COF (measured when it stabilizes) versus the size of the manganese phosphate crystal. No significant differences could be appreciated with different coatings. However, it is possible to identify a slight decrease in the COF when the crystal size is around  $16 \mu\text{m}$  corresponding to the coating deposited with  $0.3 \text{ g/L}$  of activator. This result confirms, from the viewpoint of friction, the results obtained in the wear behavior analysis. The rapid settlement occurring in the early turns of trials is consistent with that reported by Kozłowski and Czechowski,<sup>12</sup> who concluded that although the initial wear rate of phosphatized parts is greater than nonphosphatized, the settlement period is shorter. Accordingly, the phosphating increases the wear resistance during normal operation in terms of wear of the base metal.

## Conclusions

Lubricated ring-on-block tests were carried out in order to evaluate the tribological behavior of manganese phosphate coatings with different crystal sizes and, correspondingly, different available volume to retain the lubricant. Based on the results obtained, it can be concluded that:

- The manganese phosphate crystal size decreases exponentially with increasing activator concentration within the range studied (0 to  $0.7 \text{ g/L}$ ). Thickness of coatings showed the same behavior.

- An increase in the activator concentration produces higher coating uniformity, as more centers of nucleation and growth of phosphate crystals are generated.
- When the crystal size increases the available volume for accommodating lubricant also increases.
- The thickness of the coatings is a consequence of crystal size, and does not affect directly the tribological behavior.
- Under high load and low sliding speed conditions, manganese phosphate coatings with average crystal size of 16  $\mu\text{m}$  showed the best tribological performance. Such coatings present the combination of large manganese phosphate crystals (good lubricant retention) along with a good surface coverage.

This work was particularly focused in lubricated conditions, to analyze the effect of grease retention. Authors are currently working in dry condition tests to evaluate other effects.

Future lines of works should include other testing conditions, such as high or low temperature, different base materials, among others.

#### Acknowledgment

The authors acknowledge the support of Miguel Rossi from TENARIS SIDERCA.

#### Declaration of Conflicting Interests

The author(s) declared no potential conflicts of interest with respect to the research, authorship, and/or publication of this article.

#### Funding

The author(s) disclosed receipt of the following financial support for the research, authorship, and/or publication of this article: This study was supported by SGCyT-UNS and CONICET.

#### References

1. Oyamada T and Inoue Y. Evaluation of the wear process of cast iron coated with manganese phosphate. *Tribol Trans* 2003; 46: 95–100.
2. Gangopadhyay A, McWatt DG, Zdrodowski RJ, et al. Valve train friction reduction through thin film coatings and polishing. *Tribol Trans* 2012; 55: 99–108.
3. Rausch W. *The phosphating of metals*. Stevenage: Finishing Publications, 1990.
4. ASM International Handbook Committee. *ASM Handbook, Vol. 5: Surface engineering*. Materials Park, OH: ASM International, 1994.
5. Totik Y. The corrosion behaviour of manganese phosphate coatings applied to AISI 4140 steel subjected to different heat treatments. *Surf Coat Technol* 2006; 200: 2711–2717.
6. Ernens D, van Riet EJ, de Rooij MB, et al. The role of phosphate conversion coatings in make-up of casing connections. In: *SPE/IADC drilling conference and exhibition*, March 2017, Society of Petroleum Engineers. The Hague, The Netherlands.
7. Hivart P, Hauw B, Bricout J, et al. Seizure behaviour of manganese phosphate coatings according to the process conditions. *Tribol Int* 1997; 30: 561–570.
8. Hivart P, Hauw B, Dubar L, et al. Numerical identification of bulk behavior law of manganese phosphate coatings. Comparison with tribological properties. *J Coat Technol* 2003; 75: 37–44.
9. Perry J and Eyre T. The effect of phosphating on the friction and wear properties of grey cast iron. *Wear* 1977; 43: 185–197.
10. Narayanan S. Surface pretreatment by phosphate conversion coatings – a review. *Rev Adv Mater Sci* 2005; 9: 130–177.
11. Ilaiyavel S and Venkatesan A. The wear characteristics of heat treated manganese phosphate coating applied to AISI D2 steel with oil lubricant. *Tribol Ind* 2012; 34: 247–254.
12. Kozłowski A and Czechowski W. Wear resistance of manganese phosphate coatings. *Electrodepos Surf Treat* 1975; 3: 55–63.
13. Ilaiyavel S and Venkatesan A. Experimental investigation of wear characteristics on manganese phosphate coated AISI D2 steel. *Int J Precis Eng Manuf* 2012; 13: 581–586.
14. Ilaiyavel S and Venkatesan A. The wear behaviour of manganese phosphate coatings applied to AISI D2 steel subject to different heat treatment processes. *Procedia Eng* 2012; 38: 1916–1924.
15. Rasband WS. ImageJ. <http://imagej.nih.gov/ij/>
16. Schneider CA, Rasband WS and Eliceiri KW. NIH Image to ImageJ: 25 years of image analysis. *Nature Meth* 2012; 9: 671–675.
17. Khaleghi M, Gabe D and Richardson M. Characteristics of manganese phosphate coatings for wear-resistance applications. *Wear* 1979; 55: 277–287.
18. Johnson KL. *Contact mechanics*. New York: Cambridge University Press, 1987.
19. Stachowiak GW and Batchelor AW. *Engineering tribology*. 4th ed. Waltham, MA: Butterworth-Heinemann, Elsevier Inc., 2014.
20. Abbott EJ and Firestone FA. Specifying surface quality: A method based on accurate measurement and comparison. *ASME J Mech Eng* 1933; 55: 569–572.
21. MATLAB. MATLAB 2010a. Technical report, Natick, MA, USA, 2010.
22. ASTM G77-05. *Standard test method for ranking resistance of materials to sliding wear using block-on-ring*. Technical report. West Conshohocken, PA: ASTM, 2010.
23. Ay N, Çelik ON and Göncü Y. Wear characteristics of traditional manganese phosphate and composite hBN coatings. *Tribol Trans* 2013; 56: 1109–1118.